Electronic Supplementary Material (ESI) for Nanoscale.
This journal is © The Royal Society of Chemistry 2023

Supporting Information

DNA radiosensitization by terpyridine-platinum: damages induced by the 5 and 10 eV transient anions

Liangde Ouyang,[a] Hong Lin,[a] Puxiang Zhuang,[a] Yu Shao,[a] Meysam Khosravifarsani,[b] Brigitte Guérin,[b] Yi Zheng[a,b] and Léon Sanche[b]*

[a]State Key Laboratory of Photocatalysis on Energy and Environment, Faculty of Chemistry, Fuzhou University, Fuzhou 350116, P.R. China; [b]Department of Nuclear Medicine and Radiobiology, Faculty of Medicine and Health Sciences, Université de Sherbrooke, Sherbrooke, QC Canada J1H 5N4

1. Computational docking studies

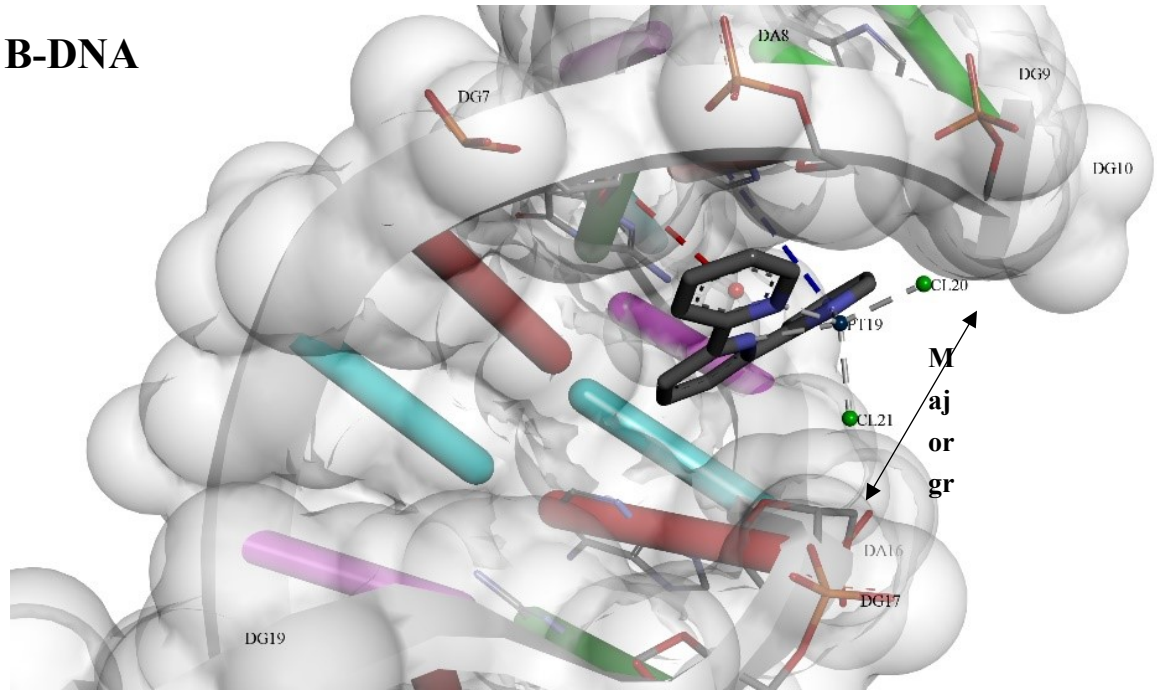

Figure 1S. Close up view of computational docking between Tpy-Pt and B-DNA DNA (CGCGAATTCGCG) (PDB ID: 1BNA) illustrating the interaction. The blue and red dash lines represent π-sigma and π-π interaction between terpyridine and purine bases (deoxyguanosine (DG7), deoxyadenosine (DA8)) whereas grey dash lines represent intramolecular bonds.

The optimal structure (PDB format) of Tpy-Pt was docked with B-DNA (PDB ID: 1BNA), taken from the protein data bank, using the HDOCK server.[1] Tpy-Pt was found to interact with DNA via the major groove (Fig. 1S) in agreement with the results of Glišic et al.,[2] who investigated theoretically and experimentally the DNA-binding properties of similar Tpy-copper(II) complexes that were explained by the planarity of the Tpy- copper(II). After energy minimization, all kinds of probable interactions between Tpy-Pt and B-DNA were visualized through Discovery Studio Visualizer (v21.0.1.20298).[3] The docking energy score for the binding was computed to be -74.5 kcal/mol^{-1}. Interestingly, the Tpy residue mainly interacts via hydrophobic π-sigma and π-π interaction with DG7 (d. 3.98 A˚) and DA8 (d. 5.5 A˚) bases, respectively. There was no interaction between Cl_2 domains and DNA bases, unlike with other traditional platinum drugs. This is consistent with previous studies that reported non-

covalent interactions of terpyridine platinum-based drugs with DNA.[2,4,5]

2. Dosimetry of ^{64}Cu–NOTA–Tpy-Pt and LEE-induced damage.

The measured lethal dose (LD_{50}) for ^{64}Cu–NOTA–Tpy-Pt was reported to be 85 ± 5 cGy within a volume equivalent to an HCT116 colorectal cancer cell of diameter 24.5 ± 3.1 μm and mass of 8.16×10^{-9} grams.[6,7] This lethal dose is at least 2.7-fold lower than that measured with low-LET gamma rays for a ^{60}Co source (2.3 ± 1.0 Gy).[6] Moreover, the activity (in MBq) from ^{64}Cu alone, required to induce 50% cell death is 28-fold higher than that for ^{64}Cu–NOTA–Tpy-Pt. Both results provide evidence for the strong radiosensitizing property of ^{64}Cu–NOTA–Tpy-Pt when bound to DNA, where any production of a high density of LEEs could be extremely effective in killing colorectal cancer cells.

The contribution to DNA damage by LEEs generated in the nucleus of HCT116 colorectal cancer cells from a dose of 85 ± 5 cGy can be obtained from the G-values for photogenerated 0-30 eV electrons interacting with plasmid DNA in a hydrated environment.[8] In a crude approximation, we can consider that 1) all secondary electrons have 10 eV (i.e., the energy of the peak in the secondary electron distribution created by high energy charge particles),[9] 2) 20 % of the deposited radiation energy goes into molecular excitation[10] and 3) the ionization potential of a cell is 10 eV. This assumption translates into 4 LEEs produced per 100 eV of energy deposited, whereas the G-value provides the number a particular damage per 100 eV. By converting the lethal dose into eV per grams and considering that the nucleus weighs 6.6 pg,[11] we estimate from a G-value of 0.203 DSBs/100 eV for LEEs[8,12] that about 29 DSBs are produce when the nucleus is exposed to a lethal dose. Furthermore, as seen from the 10-eV data in Fig. 1S, in the presence of Tpy-Pt, DSBs increase by a factor of 1.15, while other potentially lethal lesions, such as prompt and BD-related CLs and non-DSB cluster damages have yields 1.55-, 2.58-, 1.74-fold higher than that of DSBs, respectively. In other words, approximatively 200 potentially lethal lesions are created by LEEs in the nucleus, a *number that appears to be more than sufficient to kill HCT116 cells.* This estimate should be considered as a lower limit, since it neglects the specific binding of ^{64}Cu–NOTA–Tpy-Pt into the DNA structure, any damage induced outside the nucleus and SSBs occurring within 20 bp, which are usually considered as DSBs. We also took an ionization potential of 10 eV, which is too large for molecules such as DNA. Here all electrons generated in the nucleus were assumed to interact with DNA, which is not necessarily the case, but those electrons generated from other of the molecular components of the nucleus can also contribute

to DNA damage. Obviously, more detailed modelling is needed to obtain a more precise estimate the number of potentially lethal lesions generated in HCT116 colorectal cancer cells in the experiments of Khosravifarsani et al.[6]

MIRD simulations for ^{64}Cu–NOTA–Tpy-Pt corroborate the high potency of the short range (~50 and 120nm) Auger electrons[13] and the ensuing LEE distribution, indicating that translocation of the complex from the nucleus to cytoplasm in HCT116 colorectal cancer cells reduces the mean absorbed dose (Gy) to the nucleus per disintegration for cell destruction, by a factor of 14 (i.e., a reduction from 5.2×10^{-4} to 3.7×10^{-5} Gy/Bq.s).[6] On the contrary, dosimetry data indicates a very weak contribution to absorbed dose relative to the betas and positrons emitted by ^{64}Cu.[14] In other words, the role of Auger electrons in cell killing is the most significant as corroborated by the biological effectiveness (RBE) of ^{64}Cu, which is similar to that of heavy ions.[14] In conclusion, the LEEs generated by short range Auger electrons and the efficient interaction of terpyridine platinum with DNA can easily account for the large RBE value obtained by Khosravifarsani et al for the ^{64}Cu-conjugate.

3. Stability and fragility of Pt-drugs

Table 2S shows the induced damages solely due to the manipulations (i.e., from the same procedure without LEE irradiation), which can be taken to reflect DNA fragility. From these results, Tpy-Pt-DNA is found to be less fragile than cis-Pt-DNA (e.g., binding of Tpy-Pt to DNA does not alter the total conformational damage of the complex, whereas in the case of cisplatin this damage is decreased by 1.6%). This difference could be related to the weaker interaction of Tpy-Pt with DNA compared to that of cisplatin (i.e., π-π and sigma-π compared to covalent interactions, respectively). In other words, while being less damaging to DNA, Tpy-Pt-DNA adducts could still act as efficient sensitizer, which corroborates previous cell viability assays, where the weaker chemotherapeutic agent carboplatin induces a higher synergistic effect with external beam irradiation than the more cytotoxic cisplatin.[15] Additionally, the higher DNA fragility reported in table 2S in terms of CLs, SSBs, DSBs, BDs, non-DSB cluster lesions, loss of supercoiled DNA, and isolated BDs percentages for cisplatin relative to carboplatin and oxaliplatin, can be explained by different DNA bending, unwinding, and mechanism of adduct formation reported in the literature.[15,16] Previous investigations indicated a higher mutagenic effect for cisplatin relative to oxaliplatin and carboplatin.[16,17]

4. Interduplex crosslinking

Types of crosslinking possible with DNA molecules include interduplex DNA crosslinks, namely S-S, S-C, C-C, where S and C denote the supercoiled and circular configurations, respectively. Crosslinking between DNA and proteins is another possibility, but due to the high molecular weight of proteins, such crosslinks should be retained in the well of electrophoresis and not migrate in the gel. Furthermore, after purification by passing the DNA solution through a Sephadex G-50 column (see section on preparation of DNA) only a small percent of proteins is present in the sample. Considering that only a small fraction of the proteins would undergo crosslinking at low fluences, we estimate that any band due to this type of crosslink would not be detectable in our experiments. Similarly, the intensities of any bands arising from C-C or any combinations of configurations with the linear form of DNA, as well as crosslinks from reactions induced within the concatemeric forms, would not be sufficiently intense to be detected. In present study, the yields of DNA damage are measured from the initial linear portion of the exposure-response curve, i.e., the one-electron event region. Thus, even if the C band is the most intense one after the S band, the probability of a one-electron event leading to two circular forms (i.e., two single strand breaks) close to a C-C crosslink is rare, at low fluence. In conclusion, the crosslink configurations capable of producing a detectable signal are S-S and S-C, since most of the sample consists of the S form and most of transformation produce the C configuration. Finally, we note that S-S crosslinks are known to migrate close to the concatemeric position due to the similarity in configurations. The band above 10 kB in Fig. 2S is therefore most likely due to S-C crosslinks.

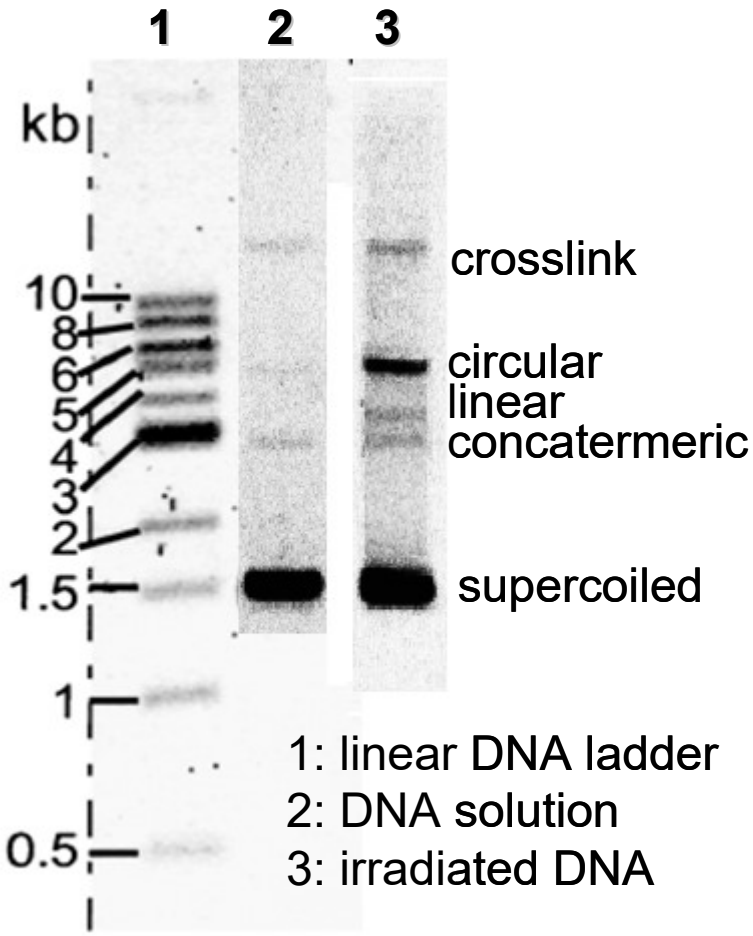

Figure 2S. The neutral agarose gel electrophoresis of pGEM-3Zf(-) plasmid DNA in solution (lane 2) and after electron irradiation (lane 3) compared to a linear-DNA reference ladder on the left (lane 1). The configuration of each band is indicated. The intensities of the bands are not normalized to each other.

5. Additional figures

Figure 3S. The UV-Visible absorption spectrum of Tpy-Pt-DNA complexes and DNA. The spectra in the range of 300 nm to 375 nm are enlarged (×10) in the insert. The characteristic absorption peaks of terpyridine are 248, 278 and 327-343 nm.

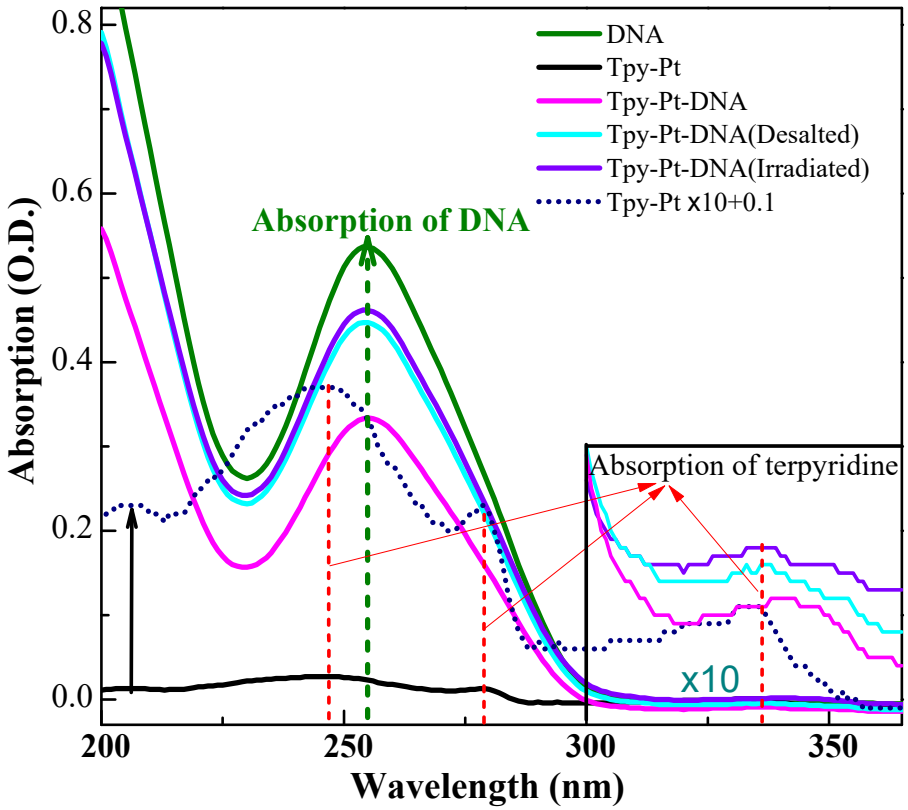

Figure 4S. Exposure-response curves for DNA damage induced by 5 eV electrons in five-monolayer films of 5:1 Tpy-Pt-DNA complexes (■) together with the curves from parallel treatment by Fpg (●) and Nth (▲) enzymes. The percentages of CLs, SSBs, DSBs and loss of supercoiled from the initial number of plasmids are shown in each frame. The dashed lines are exponential fits, and the solid lines are fits of the initial slopes. The DSBs were fitted with a linear function. Each data point is the result of 10 identical experiments and the error bars are the standard deviations of these measurements.

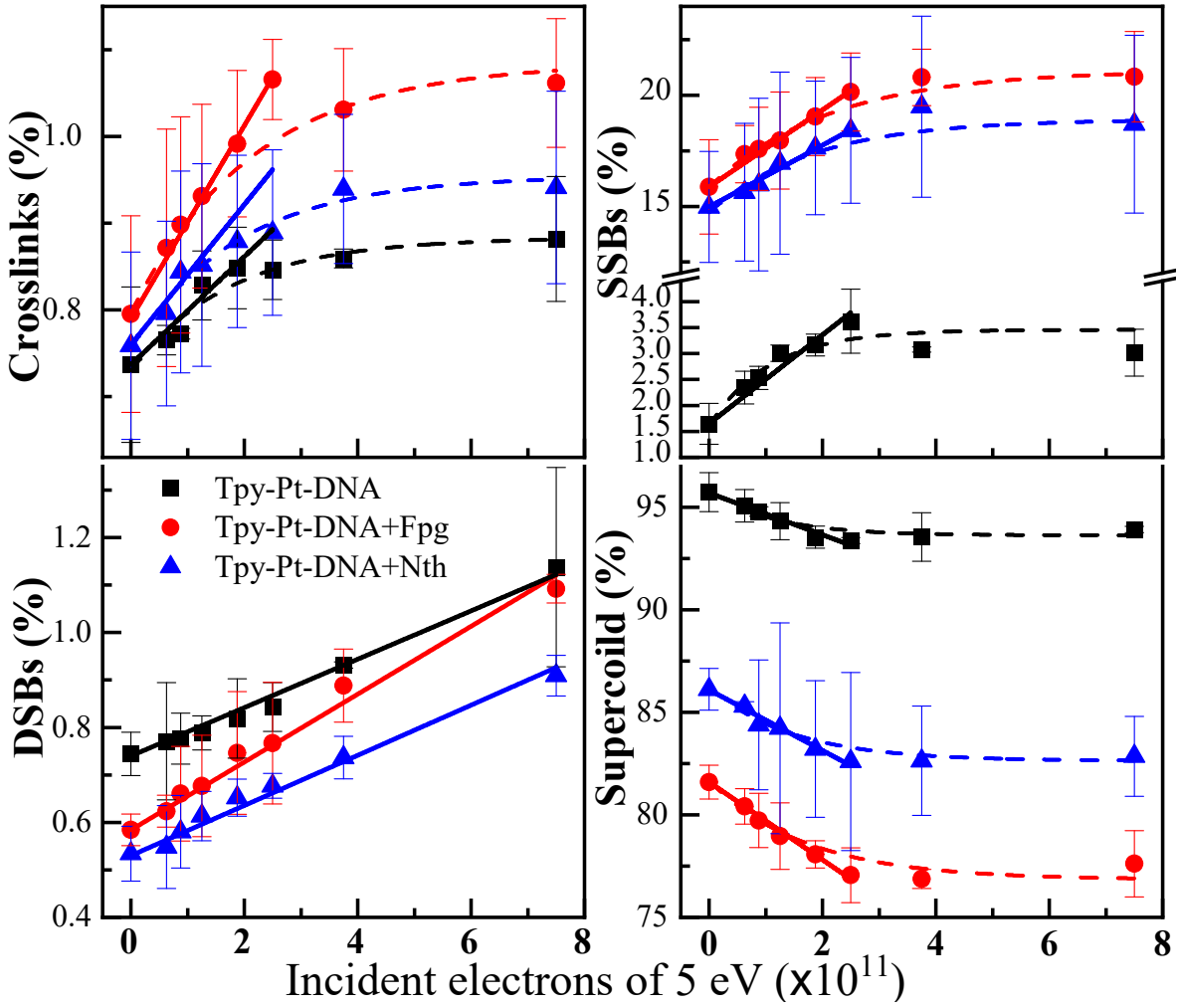

Table 1S The effective yields (in 10^{-15} electron-molecule^{-1}) of DNA damages including CLs, SSBs, DSBs, loss of supercoiled and BD related damages for Tpy-Pt-DNA complexes and DNA induced by 5 and 10 eV electrons. The errors are calculated from a linear regression fit analysis of the slope near zero fluence. The comparison results of Pt-drugs in previous studies are shown in the lower section.

Electron energy (eV)	Target	Prompt CLs	SSBs	DSBs	Loss of supercoiled	BD-related CLs	Isolated BD	Non-DSB Cluster damage	Total BDs	% of BD to total damage
5	DNA	5.6 ± 2.5	43 ± 9	3.9 ± 2.0	48 ± 6	3.6 ± 1.5	53 ± 12	3.9 ± 3.3	73 ± 25	60 ± 22
	Tpy-Pt-DNA	6.5 ± 1.5	88 ± 11	5.3 ± 1.3	106 ±17	8.8 ± 3.0	189 ± 31	4.9 ± 3.9	184 ± 38	63 ± 29
10	DNA	7.2 ± 3.1	89 ± 13	6.7 ± 2.5	104 ± 15	4.8 ± 2.2	113 ± 22	11.2 ± 2.5	113 ± 35	52 ± 20
	Tpy-Pt-DNA	11.9 ± 2.6	128 ± 18	7.7 ± 3.0	144 ± 19	19.9 ± 4.4	229 ± 42	13.4 ± 3.9	265 ± 43	65 ± 28
5	Cisplatin-DNA[15]	11 ± 4	84 ± 5	4.2 ± 1.8	109 ± 12	13 ± 6	105 ± 15	9.7 ± 2.2	136 ± 21	55 ± 13
	Cisplatin-DNA[17]	14 ± 1.1	100 ± 16.5	5.1 ± 1.0	123.6 ± 19.3					
10	Cisplatin-DNA[16]	7.2 ± 2.1	110 ± 16	3.0 ± 0.2						
	Carboplatin-DNA[16]	10.2 ± 1.6	120 ± 22	3.7 ± 0.2						
	Oxaliplatin-DNA[16]	13.5 ± 4.6	114 ± 26	2.9 ± 0.2						
	Cisplatin-DNA[15]	17 ± 5	118 ± 14	10.7 ± 4.3	168 ± 11	17 ± 5	170 ± 20	17.3 ± 4.9	200 ± 14	54 ± 7
	Cisplatin-DNA[17]	19.3 ± 2.1	136 ± 9	8.6 ± 1.1	168 ± 10					
	Cisplatin-DNA[18]	17.3 ± 4.0	137 ± 18	10.7 ± 1.3	154 ± 12	12 ± 2	165 ± 19	14.2 ± 2.4	196 ± 8	56 ± 4
	Carboplatin-DNA[18]	12.8 ± 1.0	117 ± 5	13.2 ± 1.1	136 ± 12	10.8 ± 2.5	132 ± 50	11.5 ± 2.0	159 ± 23	54 ± 9
	Oxaliplatin-DNA[18]	13.3 ± 0.4	157 ± 14	10.1 ± 1.0	173 ± 18	10.3 ± 1.9	243 ± 25	14.5 ± 2.9	261 ± 28	60 ± 8

Table 2S Percentages of cross-links, SSBs, DSBs, BDs and loss of the supercoiled configuration of the control samples (i.e., no LEE bombardment) for DNA and Pt-compounds at ratio of 5:1 lyophilized on Ta. The values in each line were obtained from the average of 10-30 samples undergoing the same treatment with the standard deviation.

Film	CLs	SSBs	DSBs	Supercoiled	BD-related CLs	Isolated BD	Non-DSB Cluster damage
DNA	0.7±0.2	1 ± 0.2	0.4±0.2	96.0 ± 0.8	0.3±0.3	10.5±2.3	0.4±1
Tpy-Pt-DNA	0.4 ± 0.1	1.2 ± 0.2	0.7 ± 0.1	96.0 ± 1.0	0.2±0.6	26.7 ± 3.6	N. D.
Cisplatin-DNA	1.6±0.3	2.5 ± 0.5	0.9±0.4	94.5 ± 0.7	0.8±0.7	21.3±4.4	1.5±1.1
carboplatin-DNA	0.4±0.1	1.7±1.3	0.1±0.1	95.5±0.8	0.2±0.3	9.5±4.2	0.3±0.3
oxaliplatin-DNA	0.3±0.1	1.6±1.1	0.1±0.1	95.6±1.7	N.D.	10.4±4.4	0.2±0.3

References

1 Y. Yan, H. Tao, J. He and S. -Y. Huang, *Nat. Protoc.*, 2020, **15**, 1829–1852.

2 B. Đ. Glišić, J. Nikodinovic-Runic, T. Ilic-Tomic, H. Wadepohl, A. Veselinović, I. M. Opsenica and M. I. Djuran, *Polyhedron*, 2018, **139**, 313-322.

3 Biovia, Discovery Studio Modeling Environment (Release 4.5.), Dassault Systèmes, San Diego, 2015.

4 S. N. Georgiades, N. H. Abd Karim, K. Suntharalingam and R. Vilar, *Angew. Chem., Int. Ed. Engl.*, 2010, **49**, 4020-4034.

5 V. S. Stafford, K. Suntharalingam, A. Shivalingam, A. J. P. White, D. J. Mann and R. Vilar, *Dalton Trans.*, 2015, **44**, 3686−3700.

6 M. Khosravifarsani, S. Ait-Mohand, B. Paquette, L. Sanche and B. Guérin, *J. Med. Chem.*, 2021, **64**, 6765–6776.

7 N. G. Durmus, H. C. Tekin, S. Guven, K. Sridhar, A. Arslan Yildiz, G. Calibasi, I. Ghiran, R. W. Davis, L. M. Steinmetz and U. Demirci, *Proc. Natl. Acad. Sci. U. S. A.*, 2015, **112**, E3661-E3668.

8 E. Alizadeh, A. G. Sanz, G. García and L. Sanche, *J. Phys. Chem. Lett.*, 2013, **4**, 820-825.

9 S. M. Pimblott and J. A. Laverne, *Radiat. Phys. Chem.*, 2007, **76**, 1244–1247.

10 Y. Hatano and M. Inokuti, in *Atomic and Molecular Data for Radiotherapy and Radiation Research*, IAEA, Vienna, IAEA-Tecdoc-799, 1995, Photoabsorption, photoionization, and photodissociation, 331-366.

11 J. F. Ward, *Prog. Nucl. Acid Res. Mol. Biol.*, 1988, **35**, 95-125.

12 E. Alizadeh and L. Sanche, *J. Phys. Chem. C.*, 2013, **117**, 22445-22453.

13 T. Kai, A. Yokoya, M. Ukai, K. Fujii and R. Watanabe, *Radiat. Phys. Chem.*, 2015, **115**, 1–5.

14 T. Kusumoto, K. Baba, S. Hasegawa, Q. Rafy and S. Kodaira, *Sci Rep.*, 2022, **12**, 8957.

15 Y. Dong, L. Zhou, Q. Tian, Y. Zheng and L. Sanche, *J. Phys. Chem. C*, 2017, **121**, 17505-17513.

16 M. Rezaee, D. J. Hunting and L. Sanche, *Int. J. Radiat. Oncol. Biol. Phys.*, 2013, **87**, 847-853.

17 Q. Bao, Y. Chen, Y. Zheng and L. Sanche, *J. Phys. Chem. C*, 2014, **118**, 15516–15524.

18 Y. Cai, L. Zhou, Y. Gao, W. Liu, Y. Shao and Y. Zheng, *ChemistrySelect*, 2019, **4**, 1084-1091.